the FEBS Journal

Unusual stability of human neuroglobin at low pH – molecular mechanisms and biological significance

Paola Picotti[1,*], Sylvia Dewilde[2], Angela Fago[3], Christian Hundahl[3], Vincenzo De Filippis[1], Luc Moens[2] and Angelo Fontana[1]

1 CRIBI Biotechnology Center, University of Padua, Italy
2 Department of Biochemistry, University of Antwerp, Belgium
3 Department of Zoophysiology, University of Aarhus, Denmark

Keywords
acid stability; globins; limited proteolysis; neuroglobin; oxygen affinity

Correspondence
A. Fontana, CRIBI Biotechnology Center, University of Padua, Viale G. Colombo 3, 35121 Padua, Italy
Fax: +39 49 8276159
Tel: +39 49 827 6156
E-mail: angelo.fontana@unipd.it

***Present address**
Institute of Molecular Systems Biology, ETH Zürich, Switzerland

(Received 16 August 2009, revised 26 September 2009, accepted 30 September 2009)

doi:10.1111/j.1742-4658.2009.07416.x

Neuroglobin (Ngb) is a recently discovered globin that is predominantly expressed in the brain, retina and other nerve tissues of human and other vertebrates. Ngb has been shown to act as a neuroprotective factor, promoting neuronal survival in conditions of hypoxic–ischemic insult, such as those occurring during stroke. In this work, the conformational and functional stability of Ngb at acidic pH was analyzed, and the results were compared to those obtained with Mb. It was shown by spectroscopic and biochemical (limited proteolysis) techniques that, at pH 2.0, apoNgb is a folded and rigid protein, retaining most of the structural features that the protein displays at neutral pH. Conversely, apoMb, under the same experimental conditions of acidic pH, is essentially a random coil polypeptide. Urea-mediated denaturation studies revealed that the stability displayed by apoNgb at pH 2.0 is very similar to that of Mb at pH 7.0. Ngb also shows enhanced functional stability as compared with Mb, being capable of heme binding over a more acidic pH range than Mb. Furthermore, Ngb reversibly binds oxygen at acidic pH, with an affinity that increases as the pH is decreased. It is proposed that the acid-stable fold of Ngb depends on the particular amino acid composition of the protein polypeptide chain. The functional stability at low pH displayed by Ngb was instead shown to be related to hexacoordination of the heme group. The biological implications of the unusual acid resistance of the folding and function of Ngb are discussed.

Introduction

Neuroglobin (Ngb) and cytoglobin (Cygb) are two proteins that have joined Mb and Hb in the vertebrate globin family [1,2]. Ngb is predominantly expressed in neuronal cells of the brain and retina [1], whereas Cygb appears to be ubiquitously expressed in human tissues [2]. Although Ngb shares little amino acid sequence similarity with vertebrate Hb (< 25%) and Mb (< 21%) [1], it displays the structural determinants of the globin fold, such as the classic three-over-three α-helical fold and all key amino acids required for ligand binding [3–5] (Fig. 1). It is of note that Ngb is characterized by the presence of an intramolecular disulfide bond, Cys46–Cys55 [6], which is unprecedented among vertebrate globins. A disulfide

Abbreviations
$[urea]_{1/2}$, urea concentration at half-transition; Cygb, cytoglobin; E/S, enzyme/substrate ratio; Ngb, neuroglobin; $pH_{1/2}$, pH at half-transition; λ_{max}, maximum absorption/emission wavelength.

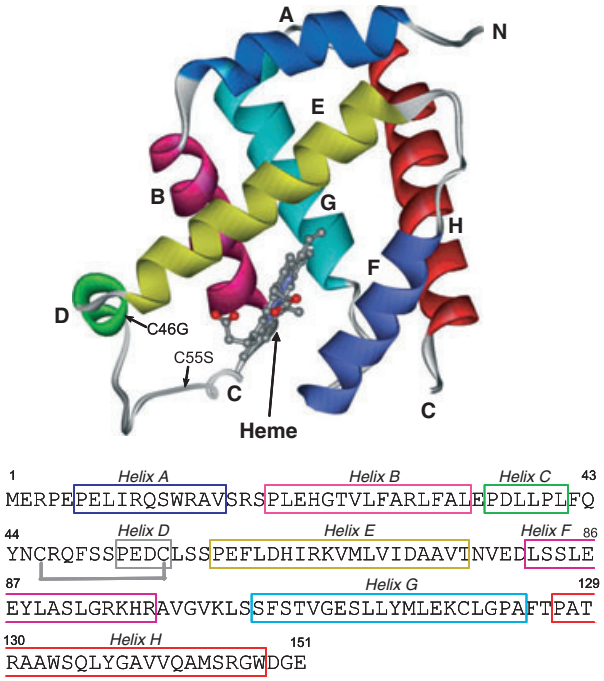

Fig. 1. Three-dimensional structure (top) and amino acid sequence (bottom) of human Ngb. The helical segments are colored in the 3D model, and are indicated by boxes in the amino acid sequence of human Ngb. The model was constructed from the X-ray structure of the Ngb mutant C46G/C55S/C120S (Protein Data Bank file 1OJ6: chain B) taken from the Brookhaven Protein Data Bank, utilizing the program WEBLAB. The location of the two Cys residues involved in the formation of the disulfide bond (Cys46–Cys55) in the wild-type protein is also indicated.

reduction–oxidation mechanism has been proposed as a means of controlling the binding and release of oxygen [6].

Spectroscopic and kinetic experiments, confirmed by crystallographic analyses, have shown that the main novel structural feature of Ngb lies in the hexacoordination of heme [3,7]. Hb and Mb in the ferrous form are normally pentacoordinated, leaving the sixth position empty and available for the binding of exogenous ligands, whereas in the ferric state they are hexacoordinated, displaying a water molecule coordinated to the heme iron [8]. By contrast, in the absence of exogenous ligands, both the ferrous and ferric forms of Ngb are hexacoordinated, with the proximal His64 being the endogenous ligand. Therefore, Ngb ligand binding requires the displacement of the intramolecular ligand His64 bound to the heme iron. Hexacoordination, which occurs in Cygb and also in bacterial and nonsymbiotic plant Hbs [9], was proposed as a novel mechanism for regulating ligand binding to the heme group in the globin family [3,9].

The physiological role and mechanism of action of Ngb and other hexacoordinated globins are under active investigation in several laboratories [10–12]. Besides the classic role of oxygen storage and supply, Ngb acts as a neuroprotective factor, conferring neuronal resistance and improving neurological outcomes in hypoxic–ischemic conditions. Similarly, the inhibition of Ngb expression increases neuronal injury upon induction of hypoxia, both *in vitro* and *in vivo* [13–16]. Interestingly, it was shown that Ngb is expressed in astrocytes [17] and that its expression in regions involved in neurodegenerative disorders declines with advancing age [18]. Clearly, an understanding of the molecular features of Ngb in dictating its biological function is of great interest, especially considering the possible implications of this protein in the pathophysiology of conditions involving cerebrovascular insults and oxidative stress, such as stroke [14,19].

For several decades, Mb, a very close relative of Ngb, has been the subject of intensive structural and functional studies with a plethora of biochemical and biophysical approaches and under a variety of physiological and denaturing conditions, becoming a paradigm of structure–function relationships of globular proteins [20,21]. In particular, apoMb (the heme-free protein) was shown to adopt partly folded states in mildly acidic solvents, and the molecular features of these states have been described in great detail, mostly by NMR measurements [22–27]. A folding intermediate occurs at pH 4.0, whereas at pH 2.0, apoMb is largely unfolded [22,26]. Clearly, it is of interest to take advantage of the wealth of structural information available for Mb and apoMb for the comparative study of the molecular features of the homologous Ngb protein. Here, we report the results of a comparative analysis of the structural and functional properties of Mb and Ngb (and the corresponding apo forms). The analysis was also extended to an Ngb mutant (H64Q) in which hexacoordination was disrupted by replacement of His64, and to an Ngb species lacking the Cys46–Cys55 disulfide bond. The results of this comparative analysis of Ngb and Mb may be used to better define the relationships between these two globins and to obtain a better understanding of the molecular features and biological function of Ngb.

Results

CD measurements

CD spectra in the far-UV region are used to analyze the secondary structure content of a protein, whereas those in the near-UV region provide information

regarding the tertiary structure of a polypeptide chain [35,36]. In this study, we conducted far-UV and near-UV CD measurements of apoNgb and apoMb dissolved in 10 mM HCl (pH 2.0), and compared them with those obtained under native conditions at pH 7.0 (Fig. 2). The far-UV CD spectrum of apoNgb at pH 2.0 displays two prominent minima at 208 and 222 nm, which are characteristic of helical polypeptides [35,36] (Fig. 2B). In contrast, at pH 2.0, apoMb displays a CD spectrum that is typical of largely unfolded polypeptides [35,36]. It is of interest that the CD spectrum of apoNgb at pH 2.0 is very similar in terms of shape and intensity to that obtained for apoNgb at pH 7.0 (Fig. 2A). Analysis of far-UV CD spectra allowed us to estimate the percentage helical content of Mb and Ngb under different conditions [29] (Table 1). At neutral pH, the α-helix content calculated for holoMb and apoMb agrees with previously reported data [37–39], whereas the content estimated for holoNgb is consistent with that (75%) deduced from the crystallographic 3D structure of the protein (Protein Data Bank file: 1OJ6) [3]. CD data indicate that, at neutral pH, the removal of the heme group induces in Mb and Ngb the same decrease in helical content (23–25%). Clearly, the CD spectra shown in Fig. 2 indicate that apoNgb does not undergo conformational changes upon a change in pH from 7.0 to 2.0, whereas apoMb almost completely unfolds at low pH.

Far-UV CD measurements at low pH were also conducted on a sample of Ngb in which the Cys46–Cys55 disulfide bond was reduced, as well as on the H64Q mutant of Ngb. In both cases, the estimated α-helical content at pH 2.0 (Table 1) was not significantly different from that of the disulfide-bonded wild-type protein. Therefore, CD data provide clear-cut evidence that disruption of the disulfide bond or replacement of the His does not alter the ability of the protein to retain a highly ordered, helical conformation at pH 2.0.

The near-UV CD spectra of apoMb and apoNgb at pH 7.0 and pH 2.0 are shown in Fig. 2C,D. The aromatic chromophores responsible for dichroic signals in the near-UV region are not conserved in the amino acid sequences of Mb and Ngb and the comparison of

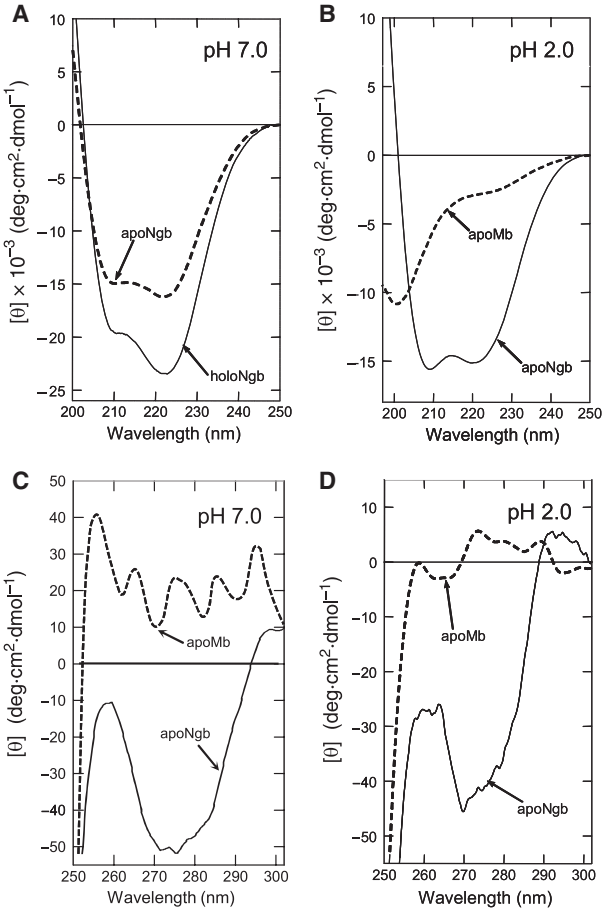

Fig. 2. CD characterization of Ngb and Mb at neutral and acidic pH. (A) Far-UV CD spectra of human holoNgb and apoNgb dissolved in 20 mM Tris/HCl and 0.15 M NaCl (pH 7.0). (B) Far-UV CD spectra of human apoNgb and horse apoMb dissolved in 0.01 M HCl (pH 2.0). (C) Near-UV CD spectra of human apoNgb and horse apoMb in 20 mM Tris/HCl and 0.15 M NaCl (pH 7.0). (D) Near-UV CD spectra of the two apoproteins dissolved in 0.01 M HCl (pH 2.0). All spectra were recorded at 25 °C.

Table 1. Spectroscopically derived structural parameters for Ngb and Mb. The figure for $pH_{1/2}$ indicates the transition midpoint of the pH-dependent heme release. The percentage of α-helical content was calculated from far-UV CD spectra and the exposure of Tyr residues from second-derivative spectra.

				Exposure of Tyr residues[a]	
Protein	$pH_{1/2}$	Conformational state	% α-Helix	% Exposure	Exposed residues
Ngb	3.2[b]	Holo, pH 7.0	72[c]	75[d]	3
		Apo, pH 7.0	47[c]	50[d]	2
		Apo, pH 2.0	44[c]	50[a]	2
Mb	4.6[b]	Holo, pH 7.0	75[d]	0.1[d]	0
		Apo, pH 7.0	52[d]	26[d]	0.5
		Apo, pH 2.0	6[c]	100[a]	2
Reduced Ngb	–	Apo, pH 2.0	43[d]		
H64Q Ngb	4.5[d]	Apo, pH 2.0	42[d]		

[a] Calculated from second-derivative spectra (Fig. 4). [b] Calculated from acid denaturation curves (Fig. 6). [c] Calculated from far-UV CD spectra (Fig. 2). [d] Spectrum or curve not shown.

the near-UV CD spectra of the two proteins is therefore not very informative. Nevertheless, the changes in the CD signals observed upon acidification are related to the conformational transitions experienced by the two proteins upon going from neutral to acid pH. At acidic pH (Fig. 2D), the near-UV CD spectrum of apoNgb essentially retains the features observed at neutral pH (Fig. 2C), with a broad negative band in the 265–285 nm region, assigned to the contributions of Phe and Tyr residues, together with a positive signal at 292 nm, characteristic of Trp residue(s) embedded in a rigid environment [35,36]. Conversely, apoMb undergoes a significant loss of tertiary structure upon lowering of the solution pH, and displays, at pH 2.0, only very weak dichroic signals in the 250–300 nm region (Fig. 2D), indicating a highly flexible polypeptide chain devoid of tertiary structure.

Fluorescence emission spectroscopy

The average polarity of the environment in which the Trp residues are embedded in apoNgb and apoMb at pH 2.0 was investigated by steady-state fluorescence emission (Fig. 3A). After excitation at 280 nm, the wavelength of maximum fluorescence intensity (λ_{max}) of apoNgb occurs at 341 nm, which is similar to the λ_{max} value observed for holoNgb at pH 7.0 (not shown). Conversely, the emission of Mb is shifted from 333 nm for the holo form at pH 7.0 (not shown) to 353 nm for the apo form at pH 2.0, which is typical of a largely unfolded polypeptide chain [40,41]. Furthermore, at variance from what observed with apoNgb, the fluorescence emission spectrum of apoMb displays the contribution of Tyr at $\sim$ 305 nm (Fig. 3A), thus indicating poor Tyr-to-Trp energy transfer, as expected for an unfolded polypeptide chain [41]. Taken together, these data indicate that the chemical environments of the three Trp residues and four Tyr residues of apoNgb at neutral pH are not appreciably altered at low pH.

Second-derivative spectroscopy

The average exposure (α) to water of Tyr residues in proteins can be estimated by second-derivative UV spectroscopy [31]. This method takes advantage of the fact that the peak-to-trough distances in the 280–295 nm region of the spectrum of proteins containing both Tyr and Trp residues are related to the polarity of the medium in which Tyr residues are embedded and, in particular, to the formation of a hydrogen bond by the hydroxyl group of Tyr [31]. The second-derivative spectra of the two apoproteins at pH 2.0 are

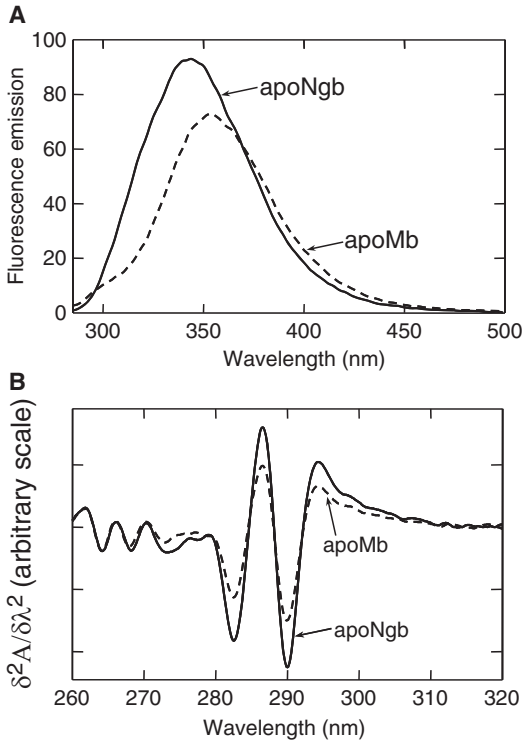

Fig. 3. Fluorescence emission and second-derivative UV absorption spectra of apoNgb and apoMb at pH 2.0. (A) Fluorescence measurements were conducted at 25 °C with the protein dissolved in 0.01 M HCl (pH 2.0). The excitation wavelength was 280 nm. (B) Second-derivative UV absorption spectra were recorded at 25 °C in 10 mM HCl (pH 2.0), for determination of the degree of exposure α of Tyr residues (see Experimental procedures). The peak-to-trough distances between the maximum at 287 nm and the minimum at 283 nm and that between the maximum at 287 nm and the minimum at 295 nm were used to calculate the Tyr exposure.

shown in Fig. 3B. The value of α was calculated for Ngb and Mb in both the holo and apo forms under neutral and acid solvent conditions (Table 1). The α-value of Tyr residues in holoNgb was calculated as 0.75, suggesting that three of the four Tyr residues of the protein are hydrogen-bonded to water or to a polar group within the protein matrix. This experimental figure for α is in agreement with the crystallographic structure of Ngb (Protein Data Bank 1OJ6: chains B and C) [3]. In fact, only Tyr137 is located in a buried and hydrophobic site; Tyr88 and Tyr115 are highly exposed on the protein surface, and Tyr44, although poorly accessible to solvent, is hydrogen-bonded to the carboxyl group of a heme propionate that provides a strongly polar environment [3]. The value of α in apoNgb is reduced to 0.50 at neutral pH, consistent with the possibility that removal of heme induces a less polar environment around Tyr44. Notably, Tyr exposure in apoNgb is essentially unchanged

on a change in pH from 7.0 to 2.0 (Table 1), in keeping with the acid resistance of the Ngb fold deduced from CD and fluorescence measurements (see above). In contrast, apoMb displays quite a different behavior from that displayed by apoNgb, reflecting a different topology of the aromatic amino acids (Fig. 3B and Table 1). In particular, with a change from neutral to acidic pH, the two Tyr residues of apoMb become completely solvent exposed (74% increase in exposure), in agreement with the largely unfolded state of apoMb at low pH [22,27].

Limited proteolysis

Proteolytic enzymes can be used for probing of protein structure and dynamics [42–45]. The rationale of this approach resides in the fact that the key parameter dictating proteolysis events is the mobility of the polypeptide chain substrate at the site of proteolysis. Consequently, partly or fully unfolded proteins are easily digested, whereas folded and native proteins are rather resistant to proteolysis [42]. In this study, proteolysis of apoNgb and apoMb was conducted with pepsin [enzyme/substrate ratio (E/S) of 1 : 100, by weight] at pH 2.0 (Fig. 4). ApoMb was shown to be cleaved very rapidly (within 75 s) at several peptide bonds along the 153 residue polypeptide chain (Fig. 4, right). Conversely, proteolysis of apoNgb, despite the broad substrate specificity of pepsin [46], is very slow and selective (Fig. 4, left). In fact, after 2 min of reaction, the large C-terminal 32–151 fragment is formed, and essentially coelutes with the intact protein from the RP-HPLC column. Whereas the initially formed N-terminal 1–31 fragment is further hydrolyzed by pepsin, the 32–151 fragment instead is resistant for hours to further proteolytic digestion, implying a folded and rigid structure of this fragment under the acidic solvent conditions of the peptic hydrolysis. Far-UV CD measurements conducted on the isolated 32–151 fragment indicated that it is still folded and highly helical even at pH 2.0 (not shown). Therefore, the proteolytic probe indicates that, at low pH, apoNgb retains a compact and rigid fold of chain region 32–151, whereas the N-teminal 1–31 portion appears to be sufficiently flexible to bind and adapt to the protease active site so that proteolysis can occur [42,43]. Conversely, the broader and much faster proteolytic cleavage of the whole polypeptide chain of apoMb (Fig. 4, right) indicates that this protein in acid solution is largely unfolded, in agreement with the results of previous spectroscopic measurements [22].

Urea-mediated denaturation

An estimate of the stability of the Ngb fold at acidic pH was obtained by measuring the urea-mediated

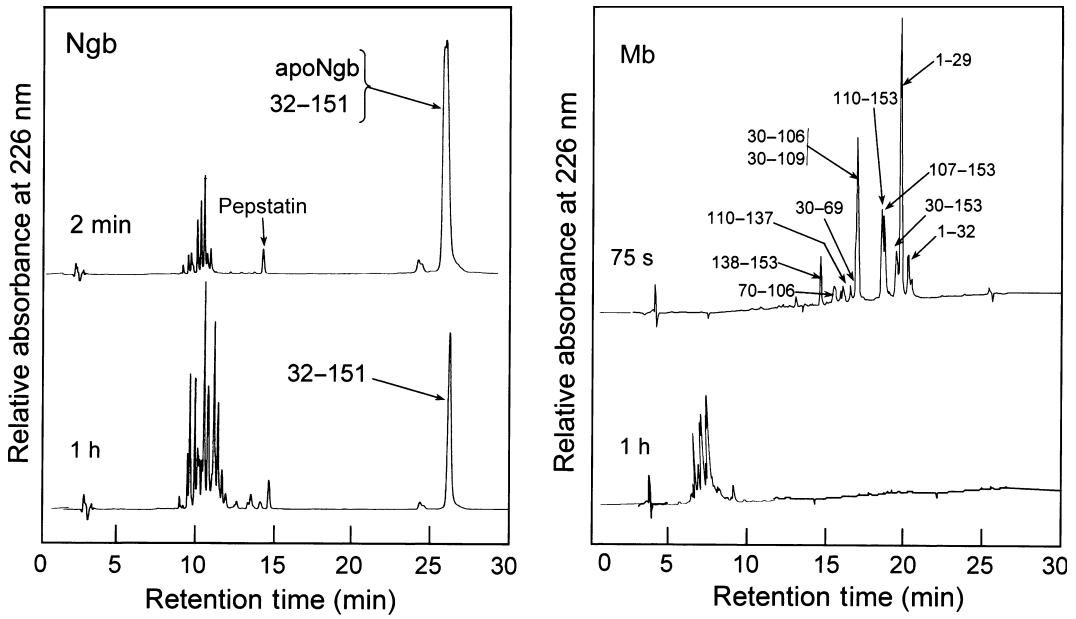

Fig. 4. Proteolysis of apoNgb and apoMb with pepsin. Proteolysis of the proteins by pepsin (E/S of 1 : 100, by weight) was conducted at 25 °C in 0.01 M HCl (pH 2.0). Left: RP-HPLC analysis of the proteolysis mixture of apoNgb with pepsin after incubation for 2 min and 1 h. Right: RP-HPLC analysis of the proteolysis mixture of apoMb with pepsin after incubation for 75 s and 1 h. The identities of the protein fragments were established by MS, and are indicated by the numbers near the chromatographic peaks.

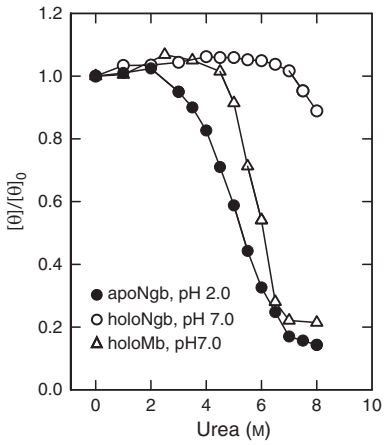

Fig. 5. Urea-mediated denaturation of Ngb and Mb. The denaturation of the proteins was monitored by recording the decrease in the ellipticity at 222 nm in the far-UV CD spectra of the protein in the presence of increasing concentrations of urea. The urea denaturation of the holo forms of Ngb (open circles) and Mb (open triangles) was performed in 20 mM Tris/HCl and 0.15 M NaCl (pH 7.0), and that of apoNgb (filled circles) was performed in 0.01 M HCl (pH 2.0). Data are expressed in terms of $[\theta]/[\theta]_0$, where $[\theta]$ is the mean residue ellipticity at a given denaturant concentration, and $[\theta]_0$ is the mean residue ellipticity in the absence of denaturant.

denaturation profile of apoNgb at pH 2.0. The unfolding of the protein was monitored by recording the mean residue ellipticity value at 222 nm, $[\theta]_{222}$, as a function of urea concentration at pH 2.0 (Fig. 5). For comparison, the urea-induced denaturation profile of holoMb at neutral pH was measured, and for this protein a urea concentration at half-transition ($[urea]_{1/2}$) of 5.5 M was observed, in agreement with previous results [47,48]. Strikingly, apoNgb at pH 2.0 showed a $[urea]_{1/2}$ value of about 5 M, which was very similar to that shown by holoMb at neutral pH. In contrast, at pH 2.0 apoMb was almost fully unfolded, even in the absence of denaturant (Fig. 2B). It is of note that holoNgb is far more stable than holoMb, as even in 8 M urea, > 85% of the helical secondary structure of the native protein was retained (Fig. 5).

pH-dependent heme release

The release of the heme group from Mb and Ngb was monitored by recording, under equilibrium conditions, the decrease in the intensity of the Soret band as a function of pH (Fig. 6). The intensity of this band is related to the molar fraction of globin-bound heme [48]. The resulting sigmoidal curve of holoNgb was characterized by a pH at half-transition ($pH_{1/2}$) of 3.2, which was about 1.4 units lower than that exhibited by Mb ($pH_{1/2}$ 4.6), indicating that the release of heme in Ngb occurs at a more acidic pH range than that observed for Mb (Table 1). In order to ascertain whether the ability of Ngb to retain heme at acidic pH was related to the hexacoordination of the heme iron, the pH dependence of heme release was also determined for the H64Q mutant of Ngb and for Cygb. The H64Q mutant, which has a pentacoordinated heme iron atom, displayed a $pH_{1/2}$ value of 4.5, which was very close to that of Mb, whereas the $pH_{1/2}$ calculated for Cygb, a hexacoordinated globin ($pH_{1/2}$ 3.3), was identical, within the limits of the experimental technique, to that of wild-type Ngb (not shown). Collectively, these data provide evidence that hexacoordination of the metal ion is a key feature in keeping the heme moiety bound to the globin structure at low pH.

Oxygen binding

Oxygen equilibrium curves for Ngb and Mb were measured at various pH values in phosphate buffer. As shown in Fig. 7, the oxygen affinity depends on the pH for Ngb but not for Mb, in agreement with previous observations [10]. A unitary slope of the Hill plot indicates absence of cooperativity, which is consistent with the monomeric structure of both proteins. It is of note that even at pH 4.7, Ngb retains the ability to bind

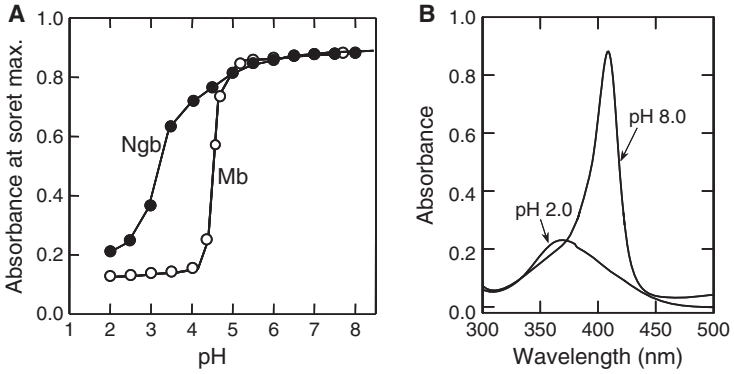

Fig. 6. Acid-induced release of heme by Ngb (filled circles) and Mb (open circles). (A) The acid-mediated denaturation was monitored by the decrease in the Soret band as a function of pH. Measurements were performed in 5 mM citrate/borate/phosphate buffer and 0.1 M NaCl, under equilibrium conditions. (B) Absorbance spectra in the Soret region of Mb at pH 8.0 and pH 2.0.

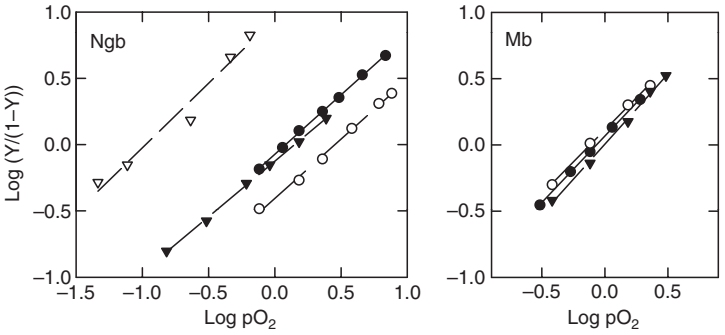

Fig. 7. Hill plots for oxygen-binding equilibria of Ngb (left) and Mb (right). Measurements were made at 25 °C in 0.1 M phosphate buffer in the presence of the enzymatic reduction system. Left: open triangles, pH 4.67; filled circles, pH 6.15; filled triangles, pH 6.35; open circles, pH 6.98. Right: filled triangles, pH 5.04; open circles, pH 6.61; filled circles, pH 6.86.

oxygen reversibly and, more importantly, it shows an increase in oxygen affinity upon lowering of the pH (oxygen tension at half-saturation at pH 4.7, 0.1 Torr). Such pH-dependent changes in affinity are not observed for Mb, which, at pH values lower than $\sim$ 5.0, starts to be denaturated and loses its oxygen-binding ability [48]. In contrast, Ngb appears to be better suited to maintain its functional features upon acidification, being still capable of reversible oxygen binding in a more acidic pH range than Mb. In previous studies, conducted on wild-type human Ngb and some mutants, it has been shown that protonation of the distal His64 in Ngb is responsible for the pH-dependent changes in the oxygen affinity of this protein [10].

Discussion

Conformational stability of Ngb

In this study, the conformational properties of human Ngb were analyzed under neutral and acidic pH conditions by a variety of spectroscopic (i.e. CD, fluorescence and second-derivative UV absorption) and biochemical (i.e. limited proteolysis and ligand binding) techniques, and compared with those of a classic prototype for protein-folding studies, horse Mb. Spectroscopic measurements at pH 2.0 were performed on the purified apo forms of Ngb and Mb, as the heme group, under these conditions, would be released in solution from the holoproteins and aggregate, reducing the quality of spectroscopic measurements. Here, we show that Ngb displays unusual acid stability as compared with that of apoMb at low pH. The acid-unfolded state adopted by apoMb at pH $\sim$ 2.0 was shown to be mostly unfolded, displaying a minimal content (at most 5%) of helical secondary structure [22,49–51]. NMR studies provided evidence that apoMb at pH 2.0 has a highly dynamic conformation, retaining local hydrophobic clusters and transient elements of secondary structure, in rapid equilibrium with fully unfolded states [22,26,27]. This view of apoMb in acid solution fits well with our spectroscopic and proteolysis data, which indicate that apoMb at pH 2.0 is mostly in a random coil conformation, lacks specific tertiary interactions, and displays an extended conformation with complete exposure of aromatic residues, and therefore can be rapidly digested by a protease. Conversely, at pH 2.0, apoNgb retains a helical secondary structure similar to that displayed at neutral pH, as well as a compact and rigid conformation that makes the protein markedly resistant to proteolytic digestion.

A systematic analysis of the effect of acid on the denaturation of 20 small monomeric proteins revealed that the exposure of a protein to an acid solution can induce a wide range of conformational changes, ranging from complete unfolding to the maintenance of an essentially native-like conformation [49–51]. Therefore, apoMb and apoNgb are at the opposite extremes of this range of acid-induced conformational change, with apoMb being completely unfolded at pH 2.0, and apoNgb showing essentially the same content of secondary structure at both pH 7.0 and pH 2.0, as well as a folded protein core with tertiary interactions. The conformational state adopted by Ngb at pH 2.0 shows even greater resistance to urea-mediated unfolding ($[urea]_{1/2}$ of 4.9 M) with respect to other acid-resistant proteins ($[urea]_{1/2}$ values ranging from 2 to 4 M) [51].

The acid resistance displayed by the Ngb fold, even though it is observed with other proteins such as T4 and chicken lysozyme, ubiquitin, and β-lactoglobulin [51], is particularly unusual among the globin family. Indeed, a variety of globins from different species (i.e. sperm whale, horse, tuna and human Mb, as well as the β-subunit of human hemoglobin) were shown to be largely unfolded at pH 2.0. Here, we have shown that the acid stability of the Ngb fold must be ascribed to the intrinsic stability of the apoprotein polypeptide chain and is not dictated by the presence of the intramolecular Cys46–Cys55 disulfide bond. Indeed, Ngb with reduced Cys residues was shown to maintain the helical fold at pH 2.0 (Table 1).

Numerous studies have indicated that globular proteins can be denatured in acid by nonspecific electrostatic repulsions between residues that become positively charged at low pH [49,51]. In addition, at low pH, some specific interactions within the protein fold, such as salt bridges, ion pairing, and hydrogen bonds, can be influenced and/or eliminated by protonation of amino acid side chains. The amino acid sequence of human Ngb, with respect to the acid-labile horse and human Mbs, displays a high degree of substitution of charged amino acids by polar but uncharged amino acids (in particular, Ser and Thr). This feature is conserved in Ngbs from other species (Fig. 8). These substitutions would reduce the number of pH-sensitive ionizable groups in the polypeptide chain of Ngb, while maintaining the overall polarity of the protein. Therefore, we propose that the decrease in the number of charged amino acids is a key determinant of the acid resistance of the Ngb fold. An analogous observation was earlier reported for the acidophilic maltose–maltodextrin-binding protein from the thermoacidophilic bacterium *Alicyclobacillus acidocaldarius*, when compared with the corresponding mesophilic protein [52].

It is of interest that, besides the unusual acid stability demonstrated here, in a recent study Ngb was shown to also possess high thermal stability, with a melting temperature (T_m) of about 100 °C [53]. The unusual stablity of Ngb to heat and protein denaturants parallels that recently observed with thermoglobin, an oxygen-binding hemoglobin isolated from the thermophilic *Aquifex aeolicus* [54].

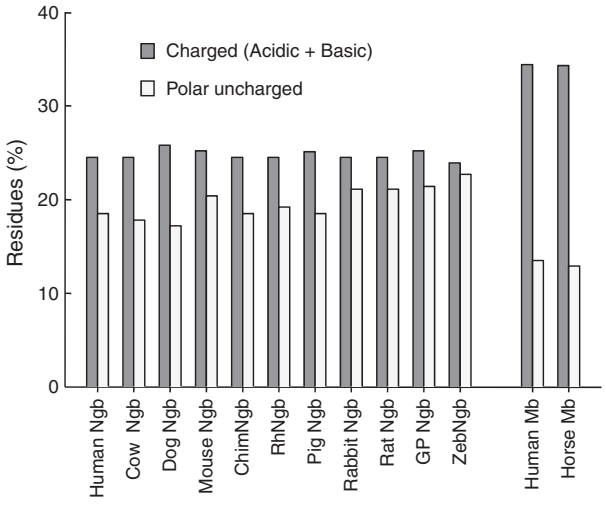

Fig. 8. Distribution of polar and charged residues in the polypeptide sequences of Ngb and Mb. The percentages of charged (basic + acidic) and polar but uncharged (Ser + Thr + Asn + Gln) residues are presented as a histogram for each protein. Chim, chimpanzee; Rh, *Rhesus macaque*; GP, green puffer; Zeb, zebrafish.

Functional stability of Ngb

The conformational stability of the apoNgb structure in acid is in agreement with the enhanced functional acid stability of the holoprotein. In fact, Ngb retains the ability to bind both heme and oxygen in a more acidic pH range than Mb. Furthermore, the oxygen affinity of Ngb increases as the pH is decreased (Fig. 7), because, at pH 4.7, the affinity is about 10-fold higher than that of Ngb and Mb at neutral pH and more than 200 times higher than that of Hb at neutral pH [55].

The heme retention capability in acid of most globins so far investigated appears to be lower than that displayed by Ngb. The acid titration curves obtained by following the decrease of the Soret band of pentacoordinated globins, such as sperm whale and horse Mb [47], porpoise Mb [56], seal Mb, and the β-subunit of human Hb [57], show $pH_{1/2}$ values ranging from 4.2 to 4.5, whereas the $pH_{1/2}$ displayed by Ngb is 3.3 (Fig. 5A). It was recently shown that, at slightly acidic pH values, substitution of the distal His residue in Ngb shifts the heme ligation mechanism of Ngb towards that of typical pentacoordinated globins [58,59]. In fact, absorption and Raman spectra of ferric H64Q Ngb below pH 6.0 revealed loss of the typical hexacoordinated His–Fe–His heme environment and indicated the presence of an iron-coordinated water molecule (His–Fe–H_2O). On this basis, we used the H64Q mutant of Ngb to test whether the heme retention capability of Ngb in acid was related to hexacoordination. The two hexacoordinated globins, Ngb and Cygb, show identical heme retention capabilities in acid ($pH_{1/2}$ 3.3), whereas the H64Q mutant shows a $pH_{1/2}$ close to that of Mb. These data collectively suggest that the heme retention ability of Ngb in acid is dependent on hexacoordination. This is in agreement with the fact that hexacoordinated bis-histidyl ferric complexes are much more stable than the pentacoordinated species [60]. Furthermore, in deoxy-Ngb, protonation of His64 implies rupture of the strongly stabilizing His64–Fe bond, which is absent in deoxy-Mb and which presumably lowers the pK_a of His64 in Ngb with respect to that of the corresponding residue in Mb. Previous studies [10] have shown that the pH dependence of oxygen affinity displayed by Ngb is lost after substitution of His64, thus implying that this residue is related to hexacoordination.

Biological implications

Ngb shows enhanced acid resistance, in terms of both protein fold and heme retention capability, to that of other globins. The stability of Ngb is even higher than that of sperm whale Mb, which has been shown to be the most stable protein among mammalian Mbs [47]. The stability of sperm whale Mb was proposed to be the result of the need for globins from deep-diving animals to be resistant to unfolding and heme loss during sustained anaerobic/acidosis conditions resulting from prolonged dives. Similarly, it can be proposed that the acid stability of Ngb is possibly related to its neuroprotective role under conditions of reduced oxygen availability, such as stroke [19]. Brain intracellular and extracellular acidosis is an important feature of cerebral ischemic–hypoxic conditions. The neuronal pH decrease upon hypoxia is associated with the switch to anaerobic glycolysis, which leads to lactic acid accumulation and increased proton liberation [61,62]. Although the degree of acidification is heterogeneous among different brain areas, it has been shown, that upon global and focal ischemia, the intraneuronal pH may fall to 6.4–6.1, and, under hyperglycemic conditions, it may reach 5.9 in neurons and 5.3 in astrocytes [61,63]. It is of note that lactate accumulation and cerebral acidosis also rapidly appear and accompany the development of common brain pathological conditions, such as Alzheimer's disease [64], traumatic brain injury and edema [65], cerebral hemorrhage [66], and pneumococcal meningitis [67], as well as solid tumor growth [68] and tissue inflammation [69]. Taken together, these observations seem to indicate that enhanced acid stability may be required by Ngb in order for it to exert its brain protective role under a variety of conditions resulting in neuronal cytosol acidification. However, the oxygen affinity of Ngb below pH 7.0 is higher than that observed with other globins, thus probably hampering the release of oxygen by Ngb under conditions of neuronal acidosis. Therefore, this observation is difficult to reconcile with the role of Ngb as an oxygen supplier to the neuron under hypoxic conditions, and prompts consideration of other mechanisms for the neuroprotective action of Ngb [10,11,70,71]. It is noteworthy that Ngb was shown to be involved in the cellular detoxification of free radicals and reactive oxygen/nitrogen species that are produced under the disease conditions listed above. Alternatively, Ngb might be a redox thiol sensor involved in a cellular signal transduction cascade, as well as a globin with enzymatic activities [11,72,73]. At present, the role of Ngb remains a matter of debate, and further studies are required to elucidate its detailed mechanism of action.

Experimental procedures

Materials

The expression and purification of human Ngb (UniProtKB accession number: Q9NPG2) and its mutants C120S and H64Q were performed as described previously [28]. Horse Mb (UniProtKB accession number: P68082) and porcine pepsin were obtained from Sigma, and the pepsin inhibitor pepstatin was purchased from Fluka. ApoNgb and apoMb were obtained from the corresponding holoproteins by removal of heme by RP-HPLC. Briefly, the holoprotein was loaded onto a C_{18} Vydac column (4.6 × 250 mm) eluted with a linear gradient of water/acetonitrile, both containing 0.05% (v/v) trifluoroacetic acid, from 5 to 40% in 5 min and from 40 to 60% in 25 min, at a flow rate of 0.8 mL·min^{-1}. The effluent was monitored by absorption measurements at 226 nm, and the fractions containing the protein were pooled and then concentrated in a SpeedVac system (Savant). The possible contamination of the apoprotein preparations by holoproteins was assessed spectrophotometrically, and no significant absorption was observed in the Soret region. In experiments conducted with the holo form of Ngb, the wild-type protein was used, whereas in those involving apoNgb, the C120S mutant of Ngb was used. The Cys120 to Ser replacement was made in order to avoid protein aggregation processes of the apoprotein due to oxidation of the free –SH group to an intermolecular disulfide bridge. A sample of reduced apoNgb, with a disrupted Cys46–Cys55 bond, was obtained by incubating the protein at 37 °C for 1 h in 50 mM Tris/HCl (pH 9.0), containing 6 M guanidinium hydrochloride and a 10-fold excess of tris(2-carboxyethyl)phosphine per mole of Cys residue of apoNgb. Purification of the reduced protein was achieved by RP-HPLC. The effective tris(2-carboxyethyl)phosphine-mediated reduction of the disulfide bond in apoNgb was confirmed by MS.

Spectroscopic measurements

CD spectra were recorded at 25 °C with a Jasco J-710 spectropolarimeter (Tokyo, Japan) equipped with a thermostatically controlled cell holder. CD measurements in the far-UV and near-UV regions were performed at protein concentrations of 0.1 mg·mL^{-1} and 0.5 mg·mL^{-1}, respectively. A 1 mm or 5 mm path-length quartz cell was used for far-UV and near-UV CD measurements, respectively. The results were expressed as mean residue ellipticity [θ] (deg·cm^2·dmol^{-1}). The percentage content of α-helical structure in proteins was estimated from far-UV CD spectra according to Scholtz *et al.* [29].

Fluorescence emission spectra were recorded at 25 °C using a Perkin-Elmer model LS-50 spectrofluorimeter,

utilizing a cuvette with a 1 cm path-length. Emission spectra were recorded in the wavelength range from 285 to 500 nm, and excitation was performed at 280 nm.

The concentration of proteins was determined from their UV absorbance at 280 nm [30], using a Perkin-Elmer Lambda-20 spectrophotometer. All spectroscopic measurements performed on Ngb and Mb (or the corresponding apo forms) were conducted in 10 mM HCl (pH 2.0) or in 20 mM Tris/HCl and 0.15 M NaCl (pH 7.0). Second-derivative UV absorption spectra were recorded at 25 °C at pH 2.0 or pH 7.0. The average exposure of Tyr residues to solvent (α) was calculated according to Ragone *et al.* [31]. This technique takes advantage of the fact that the *a/b* ratio *r* depends on the polarity of the environment in which Tyr residues are embedded. In detail, *a* is the difference in $\delta^2A/\delta\lambda^2$ between 287 nm and 283 nm, and *b* is the difference in $\delta^2A/\delta\lambda^2$ between 295 nm and 290.5 nm. The value of α was calculated with the equation $\alpha = (r_n - r_a)/(r_u - r_a)$, where r_n and r_u are the *r*-values determined for the protein under nondenaturing (i.e. 20 mM Tris/HCl, pH 7.0, 0.15 M NaCl or 10 mM HCl, pH 2.0) and denaturing (i.e. pH 7.0 or pH 2.0, containing 6 M guanidinium hydrochloride) conditions, respectively; r_a is the *a/b* value of a mixture containing the same molar ratio of Trp and Tyr as that found in the Ngb or Mb sequence, dissolved in ethylene glycol, a solvent that is thought to realistically mimic the interior of the protein matrix.

Urea-mediated denaturation

The urea-mediated denaturation of Ngb and Mb was followed by monitoring the ellipticity at 222 nm in the far-UV CD spectra of the protein (0.01 $mg{\cdot}mL^{-1}$), in the presence of increasing concentrations of urea. A 1 cm path-length cuvette (2 mL) was used for CD measurements. The protein samples were incubated at the desired denaturant concentration for 5 h at 25 °C in order to attain equilibrium. Denaturation of holoNgb or holoMb was performed in 20 mM Tris/HCl and 0.15 M NaCl (pH 7.0), and that of apoNgb was performed in 10 mM HCl (pH 2.0).

Proteolysis experiments

Limited proteolysis of apoNgb or apoMb with pepsin was performed at 25 °C with the proteins dissolved (0.5 $mg{\cdot}mL^{-1}$) in 10 mM HCl (pH 2.0), using an E/S of 1 : 100 (by weight). At time intervals, aliquots were taken from the reaction mixture, and the proteolysis was stopped by adding to the mixture the inhibitor pepstatin (enzyme/inhibitor molar ratio of 1 : 5). The proteolysis mixtures were then separated by RP-HPLC, using the experimental conditions described above. The identity of protein fragments was established by analyzing their exact masses by ESI-MS, using a Micro Q-TOF mass spectrometer (Micromass, Manchester, UK), and comparing these data with the masses calulated from the known amino acid sequence of the protein.

Heme release

The acid denaturation of Mb, Ngb and H64Q mutant of Ngb was followed by measuring the decrease in intensity of the Soret band (Ngb, λ_{max} of 412 nm; H64Q, λ_{max} of 406 nm; Mb, λ_{max} of 409 nm) in the absorption spectra of the proteins, as a function of pH. Aliquots (2–25 μL) of 1 M HCl were added to a solution (3 mL) of the protein ($\sim$ 0.1 $mg{\cdot}mL^{-1}$) in 5 mM citrate/borate/phosphate buffer (pH 8.0), containing 0.1 M NaCl. After 10 min of equilibration at 25 °C, spectra were recorded in the wavelength range 300–600 nm.

Oxygen-binding experiments

Oxygen equilibrium curves for Ngb and Mb were obtained at 25 °C in 4 μL (0.1 mM) protein samples in 0.1 M phosphate buffer, using a thin-layer equilibration chamber fed by cascaded Wösthoff gas-mixing pumps, generating precise mixtures of oxygen or air and ultrapure (> 99.998%) nitrogen, as described previously [32,33]. At each equilibration step corresponding to a given oxygen tension, the absorbance was measured with a UV–visible Cary 50 Probe spectrophotometer equipped with optic fibers [10]. Protein samples were allowed to equilibrate in phosphate buffer overnight on ice before measurements of oxygen-binding equilibria. For Ngb, an enzymatic reducing system [34] was added immediately before each experiment, in order to keep the iron atom in the ferrous oxidation state. Absorbance spectra (380–680 nm) were recorded immediately after each oxygen-binding step, to verify the absence of ferric heme. Oxygen affinity and cooperativity were obtained from the zero intercept and the slope, respectively, of Hill plots, given by log partial oxygen pressure versus $\log[Y/(1 - Y)]$, where *Y* indicates the fractional oxygen saturation.

Acknowledgements

We gratefully acknowledge the financial support of the Italian Ministry of University and Research by PRIN-2006 and FIRB Project on Protein Misfolding and Aggregation (Project No. RBNEOPX83). This work was supported also by the Danish Natural Science Research Council and the Lundbeck Foundation. We thank Professor Isabelle Mansuy of the University of Zürich for insightful discussions. PP is a recipient of a Marie Curie Intra-European fellowship and SD is a post-doctoral fellow of the Fund for Scientific Research Flanders. We are also grateful to Marcello Zambonin for his excellent technical assistance.

References

1 Burmester T, Weich B, Reinhardt S & Hankein TA (2000) Vertebrate globin expressed in the brain. *Nature* **407**, 520–523.

2 Kawada N, Kristensen DB, Asahina K, Nakatani K, Minamiyama Y, Seki S & Yoshizato K (2001) Characterization of a stellate cell activation-associated protein (STAP) with peroxidase activity found in rat hepatic stellate cells. *J Biol Chem* **276**, 25318–25323.

3 Pesce A, Dewilde S, Nardini M, Moens L, Ascenzi P, Hankeln T, Burmester T & Bolognesi M (2004) The human brain hexacoordinated neuroglobin three-dimensional structure. *Micron* **35**, 63–65.

4 Couture M, Burmester T, Hankeln T & Rousseau DL (2001) The heme environment of mouse neuroglobin: evidence for the presence of two conformations of the heme pocket. *J Biol Chem* **276**, 36377–36382.

5 Bashford D, Chothia C & Lesk AM (1987) Determinants of a protein fold: unique features of the globin amino acid sequences. *J Mol Biol* **196**, 199–216.

6 Hamdane D, Kiger L, Dewilde S, Green BN, Pesce A, Uzan J, Burmester T, bHankeln T, Bolognesi M, Moens L *et al.* (2003) The redox state of the cell regulates the ligand binding affinity of human neuroglobin and cytoglobin. *J Biol Chem* **278**, 51713–51721.

7 Trent JT III, Watts RA & Hargrove MS (2001) Human neuroglobin, a hexacoordinate hemoglobin that reversibly binds oxygen. *J Biol Chem* **276**, 30106–30110.

8 Weiland TR, Kundu S, Trent JT, Hoy JA & Hargrove MS (2004) Bis-histidyl hexacoordination in hemoglobins facilitates heme reduction kinetics. *J Am Chem Soc* **126**, 11930–11935.

9 Pesce A, Bolognesi M, Bocedi A, Ascenzi P, Dewilde S, Moens L, Hankeln T & Burmester T (2002) Neuroglobin and cytoglobin: fresh blood for the vertebrate globin family. *EMBO Rep* **3**, 1146–1151.

10 Fago A, Hundahl C, Dewilde S, Gilany K, Moens L & Weber RE (2004) Allosteric regulation and temperature dependence of oxygen binding in human neuroglobin and cytoglobin: molecular mechanisms and physiological significance. *J Biol Chem* **279**, 44417–44426.

11 Burmester T & Hankeln T (2004) Neuroglobin: a respiratory protein of the nervous system. *News Physiol Sci* **19**, 110–113.

12 Brunori M, Giuffre A, Nienhaus GU, Scandurra FM & Vallone B (2005) Neuroglobin, nitric oxide and oxygen: functional pathways and conformational changes. *Proc Natl Acad Sci USA* **102**, 8483–8488.

13 Sun YJ, Jin KL, Mao XO, Zhu YH & Greenberg DA (2001) Neuroglobin is up-regulated by and protects neurons from hypoxic–ischemic injury. *Proc Natl Acad Sci USA* **98**, 15306–15311.

14 Sun Y, Jin K, Peel A, Mao XO, Xie L & Greenberg DA (2003) Neuroglobin protects the brain from experimental stroke *in vivo*. *Proc Natl Acad Sci USA* **100**, 3497–3500.

15 Fordel E, Geuens E, Dewilde S, Rottiers P, Carmeliet P, Grooten J & Moens L (2004) Cytoglobin expression is upregulated in all tissues upon hypoxia: an *in vitro* and *in vivo* study by quantitative real-time PCR. *Biochem Biophys Res Commun* **319**, 342–348.

16 Schmidt-Kastner R, Haberkamp M, Schmitz C, Hankeln T & Burmester T (2006) Neuroglobin mRNA expression after transient global brain ischemia and prolonged hypoxia in cell culture. *Brain Res* **1103**, 173–180.

17 Chen XQ, Qin LY, Zhang CG, Yang LT, Gao Z, Liu S, Lau LT, Fung YW, Greenberg DA & Yu AC (2005) Presence of neuroglobin in cultured astrocytes. *Glia* **50**, 182–186.

18 Sun Y, Jin K, Mao XO, Xie L, Peel A, Childs JT, Logvinova A, Wang X & Greenberg DA (2005) Effect of aging on neuroglobin expression in rodent brain. *Neurobiol Aging* **26**, 275–278.

19 Venis S (2001) Neuroglobin might protect brain cells during stroke. *Lancet* **358**, 2055.

20 Antonini E & Brunori M (1970) Hemoglobin. *Annu Rev Biochem* **39**, 977–1042.

21 Perutz MF (1979) Regulation of oxygen affinity of hemoglobin: influence of structure of the globin on the heme iron. *Annu Rev Biochem* **48**, 327–386.

22 Eliezer D, Yao J, Dyson HJ & Wright PE (1998) Structural and dynamic characterization of partially folded states of apomyoglobin and implications for protein folding. *Nat Struct Biol* **5**, 148–155.

23 Yao J, Chung J, Eliezer D, Wright PE & Dyson HJ (2001) NMR structural and dynamic characterization of the acid-unfolded state of apomyoglobin provides insights into the early events in protein folding. *Biochemistry* **40**, 3561–3571.

24 Nishimura C, Dyson HJ & Wright PE (2006) Identification of native and non-native structure in kinetic folding intermediates of apomyoglobin. *J Mol Biol* **355**, 139–156.

25 Jamin M & Baldwin RL (1996) Refolding and unfolding kinetics of the equilibrium folding intermediate of apomyoglobin. *Nat Struct Biol* **3**, 613–618.

26 Gilmanshin R, Gulotta M, Dyer RB & Callender RH (2001) Structures of apomyoglobin's various acid-destabilized forms. *Biochemistry* **40**, 5127–5136.

27 Jamin M (2005) The folding process of apomyoglobin. *Protein Pept Lett* **3**, 229–234.

28 Dewilde S, Kiger L, Burmester T, Hankeln T, Baudin-Creuza V, Aerts T, Marden MC, Caubergs R & Moens L (2001) Biochemical characterization and ligand binding properties of neuroglobin, a novel member of the globin family. *J Biol Chem* **276**, 38949–38955.

29 Scholtz JM, Hong Q, York EJ, Stewart JM & Baldwin RL (1991) Parameters of helix–coil transition theory for

alanine-based peptides of varying chain lengths in water. *Biopolymers* **31**, 1463–1470.
30 Gill SC & von Hippel PH (1989) Calculation of protein extinction coefficients from amino acid sequence data. *Anal Biochem* **182**, 319–326.
31 Ragone R, Colonna G, Balestrieri C, Servillo L & Irace G (1984) Determination of tyrosine exposure in proteins by 2nd-derivative spectroscopy. *Biochemistry* **23**, 1871–1875.
32 Weber RE (1981) Cationic control of O_2 affinity in lugworm erythrocruorin. *Nature* **292**, 386–387.
33 Weber RE (1992) Use of ionic and zwitterionic (Tris, Bistris and Hepes) buffers in studies on hemoglobin function. *J Appl Physiol* **72**, 1611–1615.
34 Hayashi A, Suzuki T & Shin M (1973) Enzymic reduction system for metmyoglobin and methemoglobin and its application to functional studies of oxygen carriers. *Biochim Biophys Acta* **310**, 309–316.
35 Woody RW (1995) Circular dichroism. *Methods Enzymol* **246**, 34–71.
36 Kelly SM, Jess TJ & Price NC (2005) How to study proteins by circular dichroism. *Biochim Biophys Acta* **1751**, 119–139.
37 Goto Y & Fink AL (1994) Acid-induced folding of heme proteins. *Methods Enzymol* **232**, 3–15.
38 Lin L, Pinker RJ, Forde K, Rose GD & Kallenbach NR (1994) Molten globular characteristics of the native state of apomyoglobin. *Nat Struct Biol* **1**, 447–452.
39 Griko YV, Privalov PL, Venyaminov SY & Kutyshenko VP (1988) Thermodynamic study of the apomyoglobin structure. *J Mol Biol* **202**, 127–138.
40 Burstein EA, Vedenkina NS & Ivkova MN (1973) Fluorescence and the location of tryptophan residues in protein molecules. *Photochem Photobiol* **18**, 263–279.
41 Lakowicz JR (1986) *Principles of Fluorescence Spectroscopy*. Plenum Press, New York.
42 Fontana A, Polverino de Laureto P, Spolaore B, Frare E, Picotti P & Zambonin M (2004) Probing protein structure by limited proteolysis. *Acta Biochim Pol* **51**, 299–321.
43 Fontana A, Polverino de Laureto P, De Filippis V, Scaramella E & Zambonin M (1997) Probing the partly folded states of proteins by limited proteolysis. *Folding Des* **2**, R17–R26.
44 Fontana A, Zambonin M, Polverino de Laureto P, De Filippis V, Clementi A & Scaramella E (1997) Probing the conformational state of apomyoglobin by limited proteolysis. *J Mol Biol* **266**, 223–230.
45 Picotti P, Marabotti A, Negro A, Musi V, Sploaore B, Zambonin M & Fontana A (2004) Modulation of the structural integrity of helix F in apomyoglobin by single amino acid replacements. *Protein Sci* **13**, 1572–1585.
46 Fruton JS (1970) The specificity ad mechanism of pepsin action. *Adv Enzymol Relat Areas Mol Biol* **33**, 401–443.
47 Puett D, Friebele E & Hammonds RG (1973) Comparison of conformational stabilities of homologous hemoproteins: myoglobin from several species, human hemoglobin and subunits. *Biochim Biophys Acta* **328**, 261–277.
48 Puett D (1973) Equilibrium unfolding parameters of horse and sperm whale myoglobin: effects of guanidine hydrochloride, urea and acid. *J Biol Chem* **248**, 4623–4634.
49 Goto Y, Takahashi N & Fink AL (1990) Mechanism of acid-induced folding of proteins. *Biochemistry* **29**, 3480–3488.
50 Nishii I, Kataoka M & Goto Y (1995) Thermodynamic stability of the molten globule states of apomyoglobin. *J Mol Biol* **250**, 223–238.
51 Fink AL, Calciano LJ, Goto Y, Kurotsu T & Palleros DR (1994) Classification of acid denaturation of proteins: intermediates and unfolded states. *Biochemistry* **33**, 12504–12511.
52 Schafer K, Magnusson U, Scheffel F, Schiefner A, Sandgren MOJ, Diederichs K, Welte W, Hulsmann A, Schneider E & Mowbray SL (2004) X-ray structures of the maltose–maltodextrin-binding protein of the thermoacidophilic bacterium *Alicyclobacillus acidocaldarius* provide insight into acid stability of proteins. *J Mol Biol* **335**, 261–274.
53 Hamdane D, Kiger L, Dewilde S, Uzan J, Burmester T, Hankeln T, Moens L & Marden MC (2005) Hyperthermal stability of neuroglobin and cytoglobin. *FEBS J* **272**, 2076–2084.
54 Miranda JJL, Maillet DH, Soman J & Olson JS (2005) Thermoglobin, oxygen-avid hemoglobin in a bacterial hyperthermophile. *J Biol Chem* **280**, 36754–36761.
55 Antonini E & Brunori M (1971) *Hemoglobin and Myoglobin in their Reactions with Ligands*. North Holland Publisher Co., Amsterdam.
56 Hartzell CR, Bradshaw RA, Hapner KD & Gurd FRN (1968) Comparison of myoglobins from harbor seal porpoise and sperm whale. 2. Reactivity toward hydrogen ion and cupric ion. *J Biol Chem* **243**, 690–696.
57 Franchi D, Fronticelli C & Bucci E (1982) Folding domains as functional tools in allosteric systems: a heme-dependent domain in hemoglobin beta-subunits. *Biochemistry* **21**, 6181–6187.
58 Uno T, Ryu D, Tsutsumi H, Tomisugi Y, Ishikawa Y, Wilkinson AJ, Sato H & Hayashi T (2004) Residues in the distal heme pocket of neuroglobin: implications for the multiple ligand binding steps. *J Biol Chem* **279**, 5886–5893.
59 Nienhaus K, Kriegl JM & Nienhaus GU (2004) Structural dynamics in the active site of murine neuroglobin and its effects on ligand binding. *J Biol Chem* **279**, 22944–22952.

60 Liong EC, Dou Y, Scott EE, Olson JS & Phillips GN Jr (2001) Waterproofing the heme pocket: role of proximal amino acid side chains in preventing hemin loss from myoglobin. *J Biol Chem* **276**, 9093–9100.
61 Lipton P (1999) Ischemic cell death in brain neurons. *Physiol Rev* **79**, 1431–1568.
62 Chesler M (2005) Failure and function of intracellular pH regulation in acute hypoxic–ischemic injury of astrocytes. *Glia* **50**, 398–406.
63 Widmer H, Abiko H, Faden AI, James TL & Weinstein PR (1992) Effects of hyperglycemia on the time course of changes in energy metabolism and pH during global cerebral ischemia and reperfusion in rats: correlation of 1H and 31P NMR spectroscopy with fatty acid and excitatory amino acid levels. *J Cereb Blood Flow Metab* **12**, 456–468.
64 Yates CM, Butterworth J, Tennant MC & Gordon A (1990) Enzyme activities in relation to pH and lactate in postmortem brain in Alzheimer-type and other dementias. *J Neurochem* **55**, 1624–1630.
65 Unterberg AW, Stover J, Kress B & Kiening KL (2004) Edema and brain trauma. *Neuroscience* **129**, 1021–1029.
66 Brooke NS, Ouwerkerk R, Adams CB, Radda GK, Ledingham JG & Rajagopalan B (1994) Phosphorus-31 magnetic resonance spectra reveal prolonged intracellular acidosis in the brain following subarachnoid hemorrhage. *Proc Natl Acad Sci USA* **91**, 1903–1907.
67 Guerra-Romero L, Tauber MG, Fournier MA & Tureen JH (1992) Lactate and glucose concentrations in brain interstitial fluid, cerebrospinal fluid and serum during experimental pneumococcal meningitis. *J Infect Dis* **166**, 546–550.
68 Tannock IF & Rotin D (1989) Acid pH in tumors and its potential for therapeutic exploitation. *Cancer Res* **49**, 4373–4384.
69 Mamet J, Baron A, Lazdunski M & Voilley N (2002) Proinflammatory mediators, stimulators of sensory neuron excitability via the expression of acid-sensing ion channels. *J Neurosci* **22**, 10662–10670.
70 Wakasugi K, Kitatsuji C & Morishima I (2005) Possible neuroprotective mechanism of human neuroglobin. *Ann NY Acad Sci* **1053**, 220–230.
71 Herold S & Fago A (2005) Reactions of peroxynitrite with globin proteins and their possible physiological role. *Comp Biochem Physiol A Mol Integr Physiol* **142**, 124–129.
72 Hamdane D, Kiger L, Dewilde S, Green BN, Pesce A, Uzan J, Burmester T, Hankeln T, Bolognesi M, Moens L *et al.* (2004) Coupling of the heme and an internal disulfide bond in human neuroglobin. *Micron* **35**, 59–62.
73 Petersen MG, Dewilde S & Fago A (2008) Reactions of ferrous neuroglobin and cytoglobin with nitrite under anaerobic conditions. *J Inorg Biochem* **102**, 1777–1782.